Polar observations of solitary waves at the Earth's magnetopause

C. Cattell, J. Crumley, J. Dombeck, J. Wygant
School of Physics and Astronomy, University of Minnesota, Minneapolis, MN 55455

F. S. Mozer
Space Sciences Laboratory, University of California, Berkeley, CA 94720

ABSTRACT. Solitary waves have, for the first time, been identified in *3D* electric field data at the subsolar, equatorial magnetopause. These nonlinear, bipolar electric field pulses parallel to the magnetic field occur both as individual spikes and as trains of spikes. The solitary waves have amplitudes up to ~25 mV/m, and velocities from ~150 km/s to >2000 km/s, with scale sizes the order of a kilometer (comparable to the Debye length). Almost all the observed solitary waves are positive potential structures with potentials of ~0.1 to 5 Volts. They are often associated with very large amplitude waves in either or both the electric and magnetic fields. Although most of the observed signatures are consistent with an electron hole mode, the events with very low velocities and the few negative potential structures may be indicative of a second type of solitary wave in the magnetopause current layer. The solitary waves may be an important source of dissipation and diffusion at the magnetopause.

I. Introduction

The magnetopause is a boundary where energy conversion, mass and momentum transport, and particle acceleration and/or thermalization occur. Many of these critical processes require the existence of microphysical phenomena, for example, dissipation in reconnection. Numerous reconnection simulations (MHD, hybrid, and full particle) have been performed which indicate the importance of specific terms, such as the Hall term, electron inertia and electron pressure [see discussion in *Birn et al.*, 2001, and references therein]. However, despite many years of study, an observational answer to the question of which small-scale structures and/or waves provide the dissipation necessary to break the frozen-in condition, decoupling of the motions of ions and electrons, to allow reconnection at the Earth's magnetopause is still unresolved. *Cattell et al.* [1995], utilizing ISEE and Geotail observations of the electric field amplitudes in waves identified as lower hybrid drift waves and quasi-linear theoretical expressions for the resulting resistivity, concluded that the waves were sometimes large enough to provide the required dissipation, *consistent with the conclusions of Treumann et al. [1995] that lower hybrid waves were always able to provide sufficient resistivity*. Another process recognized to be important at the magnetopause is the diffusion needed to form the low latitude boundary layer. Recent experimental and theoretical studies [*Treumann et al.*, 1995; *Winske et al.*, 1995] in this area suggest that 'traditional' wave diffusion due to waves above the ion gyrofrequency *(with the characteristics observed by satellites to date)* may not play a major role, *although lower frequency magnetic fluctuations could provide the diffusion.*

Solitary waves, bipolar pulses in the electric field parallel to the background magnetic field, have been identified throughout the Earth's magnetosphere at narrow boundaries, such as the plasma sheet boundary [*Matsumoto et al.*, 1994; *Franz et al.*, 1998; *Cattell et al.,* 1999] and the bow shock [*Bale et al.,* 1998], and in strong currents, such as those associated with auroral acceleration region [*Temerin et al*., 1982; *Bostrom et al*., 1988; *Mozer et al*., 1997; *Ergun et al.*, 1998; *Bounds et al.*, 1999]. They have also been seen at high altitude cusp injections [*Cattell et al.*, 1999; 2001] and within the solar wind [*Magneney et al*., 1999]. Except in the ion beam regions of the auroral zone, the solitary waves are positive potential structures moving at velocities comparable to electrons (1000's of km/s) and are interpreted to be an electron hole mode, such as analytic BGK modes [*Muschietti et al*., 1999] or evolution of a bump on tail instability or electron two stream instability [*Omura et al., 1996*; *Goldman et al.*, 1999; and references therein]. Although the magnetopause is a narrow boundary with a strong current, *the signatures of ion holes or electron holes* have not, to date, been reported to occur there.

Because the dominant component of the geomagnetic field near the subsolar magnetopause is in the *northward* direction, two-dimensional instruments, which measure the component of the electric field in the *spin plane (usually the ecliptic plane)*, would not usually be able to observe solitary waves. The precession of the Polar orbit has provided a unique opportunity to observe the equatorial subsolar magnetopause with a high time resolution, fully three dimensional electric field instrument*).* In this letter, we report the discovery of solitary waves at the magnetopause in this new data set. These solitary waves may provide an important source of dissipation in the magnetopause current layer and may contribute to the diffusion of particles across the boundary to form the low latitude boundary layer.

The electric field and spacecraft potential measurements utilized herein were made by the double probe electric field instrument on the Polar satellite [*Harvey et al*., 1995] *which uses three pairs of probes, two in the spin plane (approximately the GSE x-z plane at the subsolar magnetopause) and one along the spin axis (approximately the GSE y direction).* This instrument, which saturates at ~1 V/m, obtains 3D measurements of the electric field in bursts (waveform capture) of high time resolution data. In addition to the electric field (potential difference between opposing probes), the spacecraft potential was utilized to indicate changes in density [*Pederson*, 1995]. The delay times between signals at opposing probes were examined using a cross-correlation analysis to estimate the propagation speed of electric field structures, utilizing an automatic program, which examined the parallel component of the electric field data in magnetic field-aligned coordinate system (*determined using the measured magnetic field at the highest time resolution).* The largest velocities which can be measured correspond to the resolution of the time delay and are approximately 2500 km/s. Events where no time delay could be measured are included in statistics as 'infinite velocity.' The automatic program used to calculate velocity also determines the structure width *from the velocity and the time duration* and solitary wave *potential by integrating the parallel electric field*. Note that the method yields scale sizes which are approximately a factor of 4 larger than those obtained when the potential is fit to a Gaussian because the duration of the solitary wave is based on the gradient in the parallel electric field changing sign rather than on the Gaussian half-width. *Because the solitary waves are 3D structures and the spacecraft will only rarely cut through the center of a structure, the potential amplitudes are usually underestimated.* Details of this procedure and sample cross-correlation analysis are described elsewhere [*Dombeck et al.*, 2001]. DC magnetic field data were obtained from the fluxgate magnetometers [*Russell et al., 1995*]. Solar wind parameters from ACE and WIND were obtained from the CDAWeb .

II. Observations

An example of an equatorial magnetopause crossing on 4/2/2001 at 9.4 Re and 11.6 MLT when the interplanetary magnetic field (IMF) was southward is presented in Figure 1. The transition from the magnetosphere (low density) to the magnetosheath (high density) can be clearly seen in panel a, the negative of the spacecraft potential *whose absolute value decreases as the density increases* [Pederson, 1995]. The transition is also clear in the magnetic field in geocentric solar magnetospheric (GSM) coordinates (panels b-e). The electric field waveform capture sampled at 1600 samples/s (shown in magnetic field-aligned coordinates in panels f-h) was obtained throughout the magnetopause current layer, and part of the ~34s burst extended into the magnetosheath. The waves in the perpendicular components are very large with peak-to-peak amplitudes up to more than 200 mV/m. Most of the power in the electric field is at frequencies of <50 Hz, consistent with lower hybrid waves. The search coil magnetic field data (not shown) has bursts of waves near the electron cyclotron frequency in the magnetic field minima. These waves can also be seen in the Fourier transforms of the electric field when the larger amplitude low frequency electrostatic waves and the broadband signature due to the solitary waves don't mask them. In order to see the solitary wave signatures, it is necessary to look at shorter intervals of the parallel component in the time domain data, as shown in the bottom panel *(note that the time scale is different from the upper panels)*. The typical bipolar signature can be clearly seen. There are several isolated solitary waves in addition to a train of spikes with peak-to-peak amplitudes up to 20 mV/m. The solitary wave speeds were too high for a time delay to be observable in this low data rate burst.

The top panel in Figure 2 shows the negative of the spacecraft potential and the next four panels plot the magnetic field in GSM at a magnetopause crossing, during southward IMF, on 3/12/2001 at 9.3 Re and 13.2 MLT. The top five panels cover a period of 7 minutes. The bottom panel plots 0.12 s of the parallel electric field from the ~5s waveform capture obtained at the magnetopause crossing, just prior to the location where B_z=0. Solitary waves had amplitudes of ~0.5 - 3 mV/m and velocities of ~250 km/s ->2000 km/s, northward and duskward away from the equatorial plane. All the solitary waves were moving in the same direction, and all were positive potential structures with amplitudes of ~0.1-1 V. The waves in the perpendicular components (not shown) had amplitudes up to 30 mV/m with peak power below ~100 Hz.

An example of a waveform capture obtained at a magnetopause crossing on 4/8/2001 during northward IMF is shown in Figure 3. The solar wind speed measured on ACE was ~750 km/s. The transition from the low-density magnetosphere to the high-density magnetosheath occurred near 19:06, and, at this time, the magnitude of the magnetic field reached a minimum. During this interval, the turbulence is the magnetic field maximizes. An expanded view of 0.05s of the field-aligned component of the electric field (from a 3s burst obtained at 8000 samples/s) shows a number of small amplitude (up to 4 mV/m peak to peak) solitary waves. The solitary wave velocities ranged from ~500 km/s to >2000 km/s. Approximately half were moving along the field in the northward direction, away from the equatorial plane, while the others were moving southward. Most of the solitary waves were positive potential pulses with amplitudes of ~0.1-5 V. During this crossing, several solitary waves with negative potentials occurred.

Solitary waves are observed at almost all magnetopause crossings when waveform capture data were taken. During March and April, 2001, Polar repeatedly encountered the subsolar magnetopause. There were ten cases when high time resolution waveform captures were obtained at or near the crossing. A study of these ten bursts showed that six had solitary waves that were identified by the automatic program and three others have signatures that could be identified by eye. Most waveform captures occurred on the magnetospheric side of the magnetopause current sheet or at partial crossings of the magnetopause within the magnetosphere.

III. Discussion and Conclusions

We have reported the first observations of nonlinear, bipolar electric field pulses ('solitary waves') at the Earth's magnetopause. The solitary waves have amplitudes up to 25 mV/m, and velocities from ~150 km/s to >2000 km/s. The scale sizes are the order of a kilometer, which is comparable to the Debye length for the usual range of plasma conditions at the magnetopause. Almost all the observed solitary waves are positive potential structures with potentials of ~0.1 to 5 Volts. Positive potential solitary waves moving with velocities of 1000's of km/s are consistent with electron phase space hole modes [*Muschietti et al., 1999*] which propagate at speeds comparable to the electron thermal speed. The fact that there are events that propagate at slow speeds (a few 100 km/s) and a few negative potential solitary waves may indicate that there are also other classes of solitary waves in the magnetopause current layer. The slow speeds are comparable to ion thermal speeds which suggests that some solitary waves may be ion modes [*Crumley et al., 2001*] or associated with a cold (few eV) electron population. The large spread in the observed speeds may be due to the mixture of magnetosheath, magnetospheric and ionospheric particles, which can occur in the magnetopause current layer [*Fuselier*, 1995]. *Cattell et al.* [*1999*] discussed the relationship between solitary wave speeds, the sign of the potential and possible wave modes. *Note that the wave speeds are determined in the spacecraft frame and a complete understanding of the mode of the solitary structures will require determination of the speeds in the plasma frame. The solitary wave speeds, however, are usually much faster than average speeds of either the magnetopause boundary or the plasma in this region.*

Simulations of electron phase space holes [*Omura et al., 1996*; *Goldman et al., 1999*; and references therein] demonstrate that they interact strongly with particles, resulting in particle trapping and heating. Both simulations and observations [*Carlson et al., 1998*] *of electron holes in the auroral zone* show that the electron holes result in a transfer of energy between the electron beams and the ions. Although the amplitudes of the solitary waves at the magnetopause are not as large as have been observed elsewhere in the magnetosphere (>100's mV/m), they may play an important role in anomalous processes, such as dissipation and diffusion, *because electron holes occur in large numbers and even small amplitude holes dramatically affect the electron distribution function*.

These Polar observations at the magnetopause provide strong support for the need to obtain three-dimensional measurements of the electric field, particularly at the narrow boundaries in the magnetosphere. Solitary waves have been shown to be a ubiquitous wave mode in current layers and boundaries. They are critical to an understanding of the kinetic physics of these regions. Without measurements of the out-of-the-ecliptic component of the field, solitary waves can not usually be observed at the magnetopause. This is probably the reason why previous satellites, which have observed solitary waves elsewhere in the magnetosphere (i.e. Geotail and Wind), have not reported such observations at the magnetopause. Because large amplitude waves often occur in the out-of-the-ecliptic component, the lack of *3D* measurements may provide an explanation why researchers have concluded that wave amplitudes observed at the magnetopause may be too small to provide the required anomalous transport.

Acknowledgments. The authors thank the Polar EFI engineering and software team, Dr. C. T. Russell for the use of the Polar magnetic field data, and Dr. D. Gurnett for use of the Polar search coil data. This work was supported by NASA grants NAG5-3182. J. Crumley was supported by NASA GSRP NGT5-50293.

References

Bale, S. et al., Bipolar electrostatic structures in the shock transition region: Evidence of electron phase space holes, *Geophys. Res. Lett*., **25**, 2929, 1998.

Birn, J. et al., Geospace Environmental Modeling (GEM) Magnetic Reconnection Challenge, *J. Geophys. Res*., **106,** 3715, 2001.

Bostrom, R. et al., Characteristics of solitary waves and double layers in the magnetospheric plasma, *Phys. Rev. Lett***., 61**, 82, 1988.

Bounds, S. et al., Solitary potential structures associated with ion and electron beams near 1 Re, *J. Geophys. Res*., **104**, 28709, 1999.

Cattell, C. et al., ISEE-1 and Geotail observations of low frequency waves at the magnetopause, *J. Geophys. Res.* **100**, 11823, 1995.

Cattell, C. et al., Observations of large amplitude parallel electric field wave packets at the plasma sheet boundary, *Geophys. Res. Lett*., **25**, 857-900, 1998.

Cattell, C. et al., Comparisons of Polar satellite observations of solitary wave velocities in the plasma sheet boundary and the high altitude cusp to those in the auroral zone, *Geophys. Res. Lett*., **26**, 425-428, 1999.

Cattell, C. et al., Comparison of solitary waves and wave packets observed at plasma sheet boundary to results from the auroral zone, in *Phys. And Chem. of the Earth*, in press, 2000.

Crumley, J., C. Cattell and R. Lysak, and J. Dombeck, Studies of ion solitary waves using simulations including hydrogen and oxygen beams, *J. Geophys. Res*., **106**, 6007, 2001.

Dombeck, J., C. Cattell, J. Crumley, W. Peterson, H. Collin, and C. Kletzing, Observed trends in auroral zone ion solitary wave structure characteristics using data from Polar, *J. Geophys. Res*., in press, 2001.

Ergun, R. et al., FAST satellite observations of large-amplitude solitary wave structures, *Geophys. Res. Lett*., **25**, 2041-2044, 1998.

Franz, J., P. Kintner, and J. Pickett, Polar observations of coherent electric field structures, *Geophys. Res. Lett*., **25**, 1277-1280, 1998.

Franz, J., P. Kintner, and J. Pickett, On the perpendicular scale size of electron phase space holes, *Geophys. Res. Lett*., **27**, 169-172, 2000.

Fuselier,S., Kinetic aspects of reconnection at the magnetopause, in *Physics of the Magnetopause*, Geophys. Mon. **90**, AGU P. Song, B. Sonnerup and M. Thomsen, eds., pg. 181, 1995.

Goldman, M., M. Oppenheim, and D. Newman, Nonlinear two-stream instabilities as an explanation for auroral biploar wave structures, *Geophys. Res. Lett*., **26**, 1821-1824, 1999.

Harvey, P. et al., The Electric Field Instrument on the Polar Satellite, in *The Global Geospace Mission*, C.T. Russell, ed., p. 583, 1995.

Mangeney, A., et al., WIND observations of coherent electrostatic waves in the solar wind, *Annales Geophysicae*, **17**, 307, 1999.

Matsumoto, H. et al., Generation mechanism of ESW based on the GEOTAIL Plasma Wave Observation, Plasma Observation and Particle Simulation, *Geophys. Res. Lett*., **26**, 421-424, 1999.

Mozer, F. et al., New features in time domain electric field structures in the auroral acceleration region, *Phys. Rev. Lett.*, **79**, 1281, 1997.

Muschietti, L. et al., Phase-space electron holes along magnetic field lines, *Geophys. Res. Lett*., **26**, 1093, 1999.

Omura, Y. et al., Electron beam instabilities as the generation mechanism of electrostatic solitary waves in the magnetotail, *J. Geophys. Res*, **101**, 2685-2697, 1996.

Pedersen, A., Solar wind and magnetospheric plasma diagnostics by spacecraft electrostatic potential measurements, *Annales Geophysicae*, **13**, 118 1995.

Russell, C. T. et al., The GGS/Polar Magnetic Fields Investigation, in *The Global Geospace Mission*, C.T. Russell, ed., p. 563, 1995.

Temerin, M. et al., Observations of solitary waves and double layers in the auroral plasma, *Phys. Rev. Lett.*, **48**, 1175, 1982.

Treumann, R., J. LaBelle and T. Bauer, Diffusion Processes: An Observational Perspective, in *Physics of the Magnetopause*, Geophys. Mon. **90**, AGU P. Song, B. Sonnerup and M. Thomsen, eds., pg. 331, 1995.

Winske, D., V. Thomas and N. Omidi, Diffusion at the Magnetopause: A Theoretical Perspective, in *Physics of the Magnetopause*, Geophys. Mon. **90**, AGU P. Song, B. Sonnerup and M. Thomsen, eds., pg. 321, 1995.

Figure Captions

Figure 1. A magnetopause crossing on 4/2/2001. From top to bottom the panels are: The negative of the spacecraft potential; the magnitude of the magnetic field and the three components of the magnetic field in GSM; the three components of the electric field *in magnetic field-aligned coordinates (z along the field)* during the waveform capture; and an expanded view of the field-aligned component of the electric field for 0.12s to show an example of the solitary waves.

Figure 2. A magnetopause crossing on 3/12/2001. From top to bottom the panels are: The negative of the spacecraft potential; the magnitude of the magnetic field and the three components of the magnetic field in GSM; and an expanded view of the field-aligned component of the electric field for 0.12s to show an example of the solitary waves.

Figure 3. A magnetopause crossing during northward IMF on 4/8/2001 (same format as Fig.2).

Figure 1. A magnetopause crossing on 4/2/2001. From top to bottom the panels are: The negative of the spacecraft potential; the magnitude of the magnetic field and the three components of the magnetic field in GSM; the three components of the electric field *in magnetic field-aligned coordinates* during the waveform capture; and an expanded view of the field-aligned component of the electric field for 0.12s to show an example of the solitary waves.

Figure 2. A magnetopause crossing on 3/12/2001. From top to bottom the panels are: The negative of the spacecraft potential; the magnitude of the magnetic field and the three components of the magnetic field in GSM; and an expanded view of the field-aligned component of the electric field for 0.12s to show an example of the solitary waves.

Figure 3. A magnetopause crossing during northward IMF on 4/8/2001 (same format as Fig.2).

C. A. Cattell, J. Dombeck and J. R. Wygant, School of Physics and Astronomy, 116 Church St. SE, University of Minnesota, Minneapolis, MN 55455 (e-mail: cattell@belka.space.umn.edu)

F. S. Mozer, Space Sciences Laboratory, University of California, Berkeley, CA 94720

(Received Sept. 2001; revised ******;
accepted ******)

CATTELL ET AL: MAGNETOPAUSE SOLITARY WAVES

CATTELL ET AL: MAGNETOPAUSE SOLITARY WAVES

CATTELL ET AL: MAGNETOPAUSE SOLITARY WAVES

POLAR 2001/04/02 (Day 92), 00:20:22 – 00:22:20

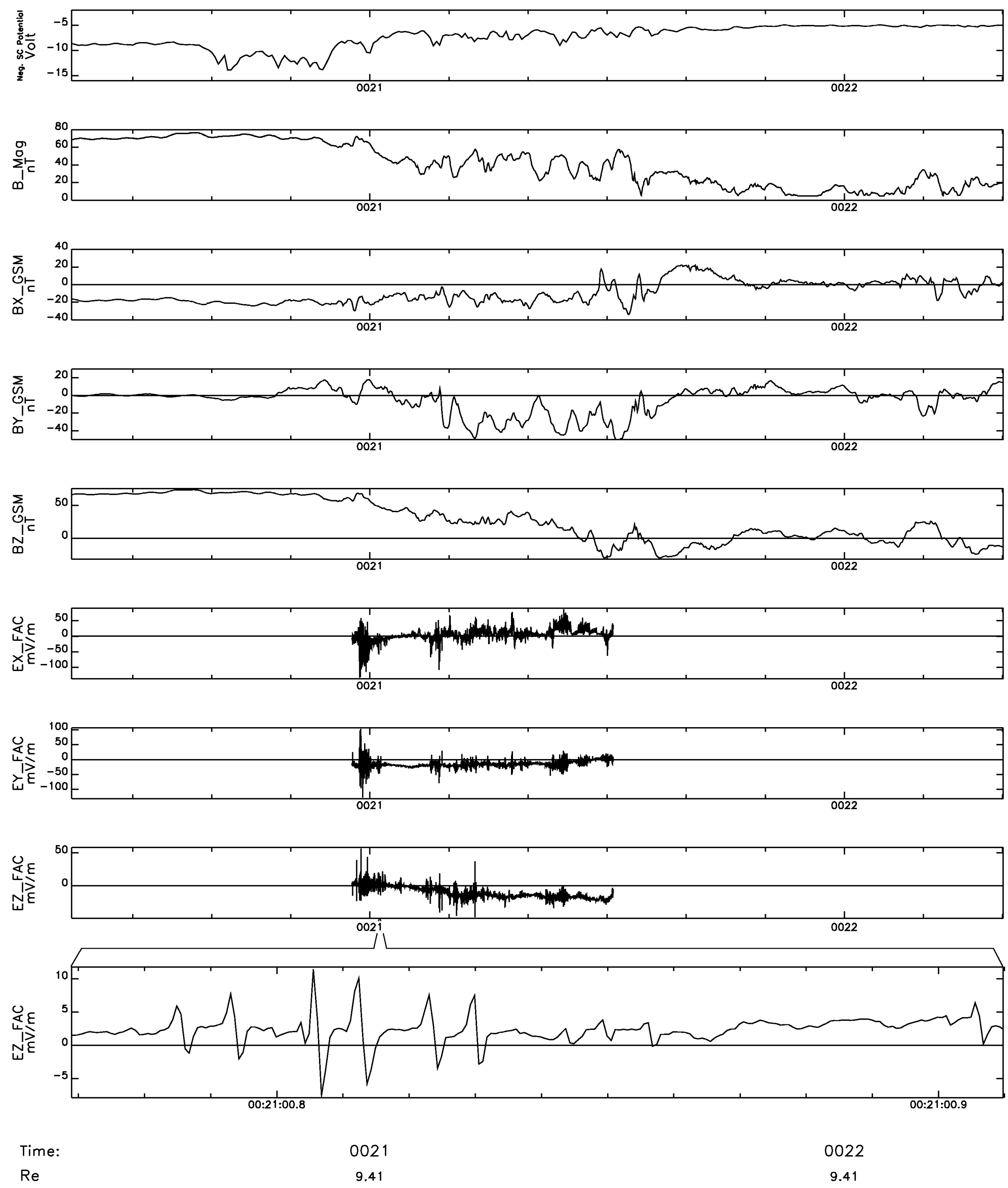

Time:	0021	0022
Re	9.41	9.41
MLT	11.59	11.59
MLat	12.08	12.12
LShell	9.77	9.78

P:<SDT>, V:<2.4> T:<Thu Aug 30 13:54:48 2001>; Cfg=magnetopause_fig1_12mar

POLAR 2001/03/12 (Day 71), 11:44 - 11:51

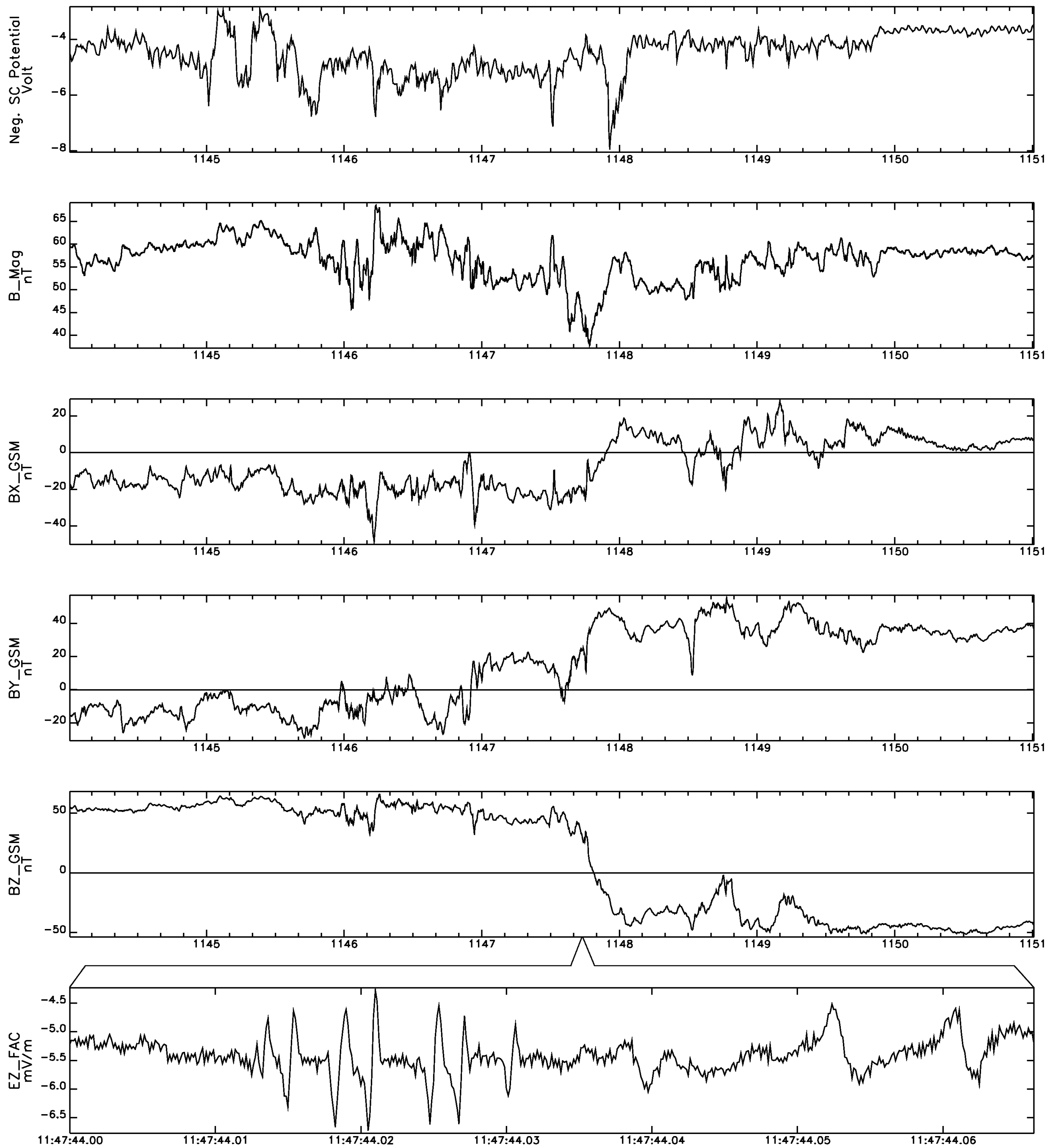

Time:	1145	1146	1147	1148	1149	1150	1151
Re	9.32	9.33	9.33	9.33	9.34	9.34	9.34
MLT	13.17	13.17	13.17	13.17	13.17	13.18	13.18
MLat	15.98	16.11	16.23	16.35	16.47	16.59	16.71
LShell	10.13	10.15	10.17	10.18	10.20	10.22	10.23

P:<SDT>, V:<2.4> T:<Mon Aug 27 13:23:12 2001>; Cfg=magnetopause_fig1_12mar

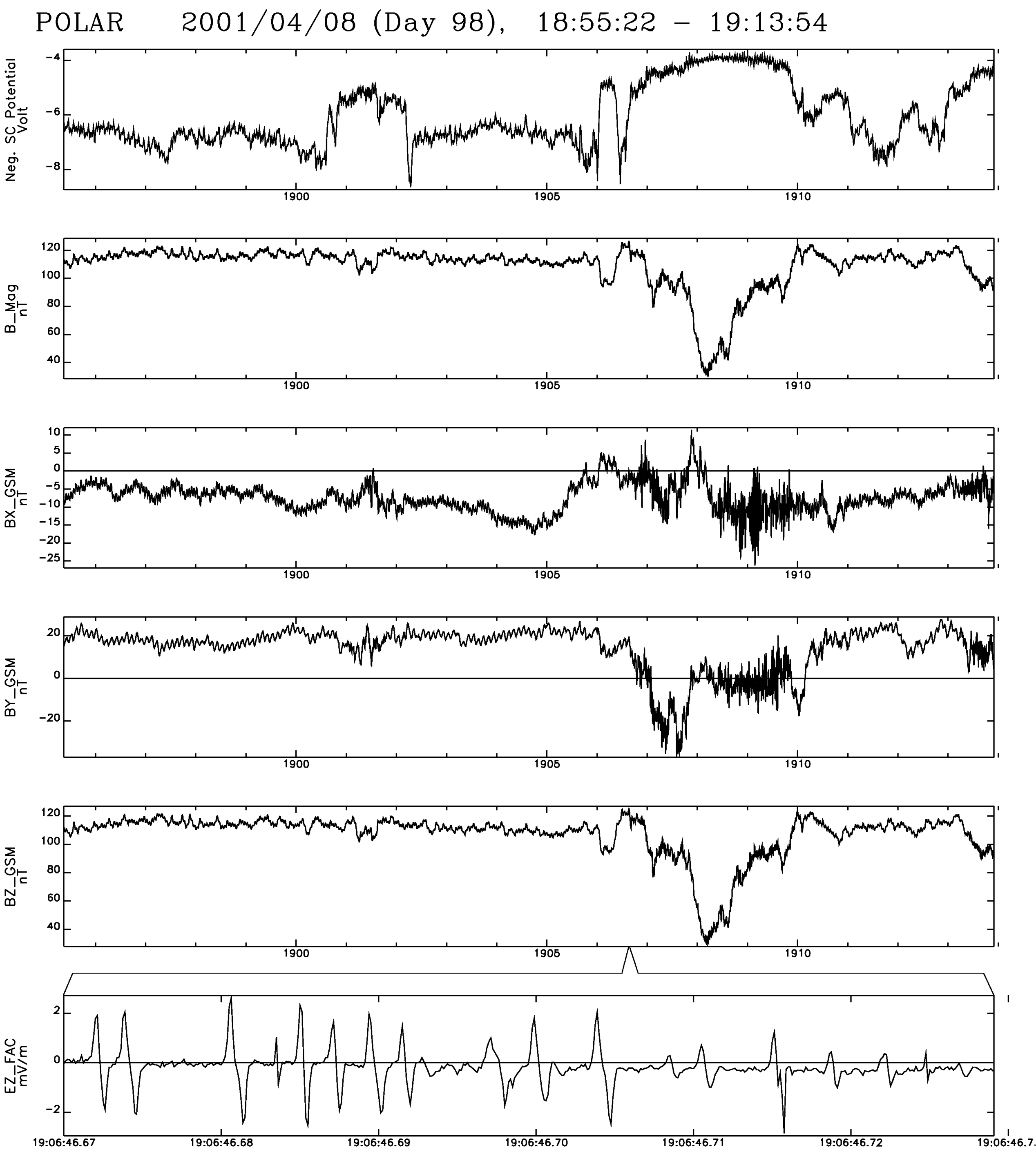

Time:	1900	1905	1910
Re	8.72	8.76	8.80
MLT	11.22	11.22	11.22
MLat	13.93	14.22	14.51
LShell	9.28	9.34	9.41

P:<SDT>, V:<2.4> T:<Thu Aug 30 13:54:48 2001>; Cfg=magnetopause_fig1_12mar